SEVENTH INTERNATIONAL CONFERENCE ON THERMOELECTRIC ENERGY CONVERSION

THE UNIVERSITY OF TEXAS AT ARLINGTON
March 16-18, 1988

PROCEEDINGS OF THE SEVENTH INTERNATIONAL CONFERENCE ON THERMOELECTRIC ENERGY CONVERSION

Rosebud Theater
University Center
The University of Texas at Arlington
Arlington, Texas
March 16-18, 1988

Sponsored by
The Department of Electrical Engineering
The University of Texas at Arlington

PROCEEDINGS OF THE SEVENTH INTERNATIONAL CONFERENCE ON THERMOELECTRIC ENERGY CONVERSION

EDITOR: K.R. RAO, Ph.D.

CPS-6-88-Rev

ACKNOWLEDGEMENTS

The editor would like to thank the authors, session chairmen and panelists for their cooperation and contributions. Special thanks to Evanita Bickle, Phan Phuong Lam, Doan Hien Bui for ably handling the extensive correspondence with authors and other participants. The editor acknowledges the help and assistance of Dr. Jack Fitzer, Dr. Floyd Cash, Joe Yeal Nam, Miran Mohammed, Majid Chelemal, Sekhavat Sharghi, Sue Fox, Donna High, Sue Knight, and the Arlington Convention and Visitor's Burearu during all phases of this conference. The patience and understanding of his wife, Karuna, regarding the conference is appreciated. Special thanks to Vernice Franks for providing the Rosebud Theater and its facilities.

TABLE OF CONTENTS

Author Index

Author Index

THE THERMOTUNNEL CONVERTER: A HYBRID THERMOELECTRIC/THERMIONIC DEVICE.*

Fred N. Huffman - Thermo Electron Corp., Waltham, MA

Zia Haq - Energetics Inc., Columbia, MD

ABSTRACT

The thermotunnel converter (TTC) is an innovative energy conversion device that utilizes the principle of electron tunneling to convert thermal energy into electricity. The TTC consists of a series of hot emitter surfaces spaced about 10 Å away from cooler collector surfaces. An analytical model indicates that the TTC would operate efficiently in the temperature range from 300 to 1500 K. Highly oriented pyrolytic graphite (HOPG) intercalated with cesium is an appropriate material for making a practical TTC. Extrapolation of potassium intercalated HOPG data to temperatures of 800 - 1500 K indicate that intercalated HOPG has attractive thermoelectric properties at these conditions.

THE TUNNELING CONCEPT

The thermotunnel converter (TTC) is a new direct energy conversion device that has characteristics in common with thermionic and thermoelectric converters. The thermotunnel converter operates at lower temperatures than thermionic converters, and initial calculations suggest that greater conversion efficiencies may be obtainable from a TTC than from existing thermoelectric and thermionic converters.

The thermotunnel converter (TTC) consists of a hot plate, called an emitter, spaced close to a cooler plate, called the collector. To this extent it is similar to a thermionic converter. The fundamental difference is that the emitter-collector spacings of a TTC are on the order of 10 Å, compared to typical vacuum-close spaced thermionic converter spacings of 0.001 cm. In the TTC, due to spacings on the order of atomic dimensions, all electrons above the Fermi level have some probability to quantum mechanically tunnel through the potential barrier. Essentially the thermotunnel converter is a heat engine in which a fraction of the heat flux through the emitter is expended in raising electrons to energy levels where the probability of tunneling through the potential barrier is increased.

Tunneling is a manifestation of the Heisenberg uncertainty principle, which implies that an electron exists in a cloud surrounding the nucleus. Given enough energy, and a sufficiently small potential barrier, there is a probability of finding the electron on either side of the barrier. The imposition of a temperature difference across an emitter and collector surface allows us to utilize tunneling for the purpose of energy conversion. The temperature difference ensures that the number of electrons tunneling from the emitter to collector is greater than the number of electrons tunneling back from the collector to the emitter. Hence the thermal gradient acts as a driving force that generates a net current which can be utilized through a load.

Some physical insight may be gained by examining Figure 1. The Fermi function gives the probability that an allowed state in dE about E will be occupied at the given temperature. Hence over a restricted range around the Fermi level energy, the cross hatched area is proportional to the number of electrons tunneling from the emitter to collector contributing to the current through the device whereas the shaded area is proportional to the number of electrons from the collector to the emitter subtracting from the current through the device. The higher energy electrons (i.e. those in the cross-hatched area) are much more likely to tunnel than the lower energy electrons (i.e. those in the shaded area). Therefore, for TE > TC there will exist a net current across the electrodes provided the output voltage, V, is less than the open circuit voltage, Voc.

ANALYTICAL MODEL OF THERMOTUNNEL CONVERTER

An analytical model has been developed which predicts the performance characteristics of a thermotunnel converter device. The model assumes a potential diagram in a thermotunnel converter as shown in Figure 2. For a first approximation a linear potential barrier is assumed, and the emitter and collector work functions are considered to be equal. Penetration coefficients for the one dimensional potential barrier can be found in the Wentzel- Kramers-Brillouin (WKB) approximation (Ref. 1, 2, 3).

$$D(E_x) = \exp[(-4\pi s/h)\{2m(E_F+\phi-\varepsilon V/2-E_x)\}^{\frac{1}{2}}]$$

where
- s = barrier width
- h = Plancks constant
- m = electron rest mass
- E = energy level of electron
- ø = material work function
- E_F = Fermi energy level
- V = voltage induced by current flow

The net electron flux through the thermotunnel converter is found by subtracting the electron flux penetrating the barrier from the collector to the emitter from the electron flux penetrating the barrier from the emitter to the collector. With proper representation of these quantities as well as an appropriate coordinate change from rectangular to polar coordinates, it can be shown that the net current density in the TTC is given by

$$J = \left(\frac{4\pi me}{h^3}\right) \int_0^\infty D(E_x)\, Y(E_x)\, dE_x \qquad (1)$$

* Sponsored by U.S. Department of Energy, Small Business Innovation Research Contract No. DE-AC05-86ER80389.

where

$$Y(E_x) = \int_{E_x}^{\infty} \{f[E,E_F,T_E]-f[E,(E_F+eV),T_C]\}dE$$

and D(E) is the same as before. The Fermi function is given by

$$f(E) = 1/[\exp\{(E-E_F)/kT\}+1]$$

where k = Boltzmanns constant
T_E = emitter temperature
T_C = collector temperature

The existing research on tunneling phenomenon has concentrated on low temperature regimes (< 300 K). In all cases the tunneling junction measurements of current density and voltage are made under isothermal conditions. In some cases a bias potential is imposed on the tunneling junction which causes the output current density to increase with increasing bias potential. Our analysis has taken into account the high-temperature operation, and the imposition of a temperature gradient across the device. In addition, no external bias potential is imposed the TTC, and only the voltage generated by electron transport is calculated with the above equations.

A FORTRAN program has been written which calculates the TTC device net current density by numerically integrating Equation 1. Simpsons composite algorithm is applied over the limits of integration to arrive at the value of J. All calculations are performed in double precision format to minimize roundoff error.

The calculated current density - voltage characteristics (shown in Figure 3) indicate that a significant power density can be obtained from such a device with temperature difference of 800 K - 300 K between the emitter-collector surfaces. Thermionic converters exhibit similar J-V response curves, but at much higher temperatures (greater than 1600 K).

Along with the current density, an important thermotunnel converter parameter is efficiency. The efficiency equation for a thermotunnel converter is

$$\eta = \frac{J\left[V - \frac{J\rho\ell}{S_A} - \bar{\alpha}(T_E - T_C)\right]}{\frac{4\pi me}{h^3}\int_0^{E_m}(E_x - E_{FE})D(E_x)dE_x \int_{E_x}^{\infty} f[T_E]dE - \frac{4\pi me}{h^3}\int_0^{E_m}(E_x - E_{FE})D(E_x)dE_x \int_0^{\infty} f[T_C]dE + Q_R + Q_L + Q_S}$$

where ρ = resistivity of conductor
ℓ = length of conductor lead
S_A = cross section per unit tunnel area of conductor
$\bar{\alpha}$ = mean thermoelectric power of conductor lead
Q_S = conduction heat loss
Q_R = radiation heat loss
Q_L = lead loss

In the numerator, the lead loss in the conductor and thermoelectric emf due to the temperature difference have been subtracted from the output voltage. Hence, the numerator represents the useful output power density. The first term in the denominator accounts for the power expended in lifting electrons from the emitter Fermi level to the E_x level where they will tunnel, while the second term in the denominator is the power returned to the emitter by electrons tunnelling from the collector to emitter. Q_C, Q_R, and Q_L represent the thermal losses due to spacer conduction, radiation, and lead conduction. The TTC efficiency expression is analogous to that for the thermionic converter. The variation of efficiency as a function of output voltage, parametric in emitter temperature, is shown in Figure 4.

INTERCALATION COMPOUND EXPERIMENTAL DATA EXTRAPOLATION

The thermotunnel converter is predicated on several requirements: (1) multiplicity of extremely close-spaced electrodes, (2) reduced heat loss by thermal conductivity through the TTC material, and (3) low work function material to facilitate electron transport. The concept of the thermotunnel converter can only now be translated into practice due to recent advances in the field of material science. It is possible to "chemically" space materials on the order of 10 Å apart by intercalation. Intercalation compounds are formed by inserting dopant molecules into the lattice structure of a host material. Graphite is a host material that readily forms intercalation compounds. The structure of pure and intercalated graphite is illustrated in Figure 5. Pristine graphite layers are spaced 3.35 Å apart. The intercalant atoms or molecules orient themselves in between the graphite layers thus increasing the adjacent carbon layer distances up to about 20 Å depending on the size of the intercalant species. The "stage" of a compound is the number of carbon layers between adjacent intercalant layers. Intercalated compounds exhibit well defined chemical compositions with physical and chemical properties dramatically different from the original host material. Lattice transport properties are a strong function of interatomic spacing, and intercalation causes the host atoms to be spaced further apart, thus causing significant reductions in thermal conductivity. Graphite intercalation compounds (GIC) with cesium as the intercalant appears to be the most suitable material for the thermotunnel converter.

Although there has been an explosion of GIC investigations over the past decade, few of them are directly relevant to the question of using GIC's as intermediate temperature energy conversion materials. Only one material, Stage-5 Potassium-GIC, could be found for which the three thermoelectric properties (i.e., thermopower, electrical resistivity, and thermal conductivity) had been measured. Even in this case, the measurements were only available at low temperature conditions (< 300 K).

The few thermoelectric data that are available have been extrapolated to ascertain if there is an experimental basis, independent of theory, for expecting GIC materials to provide improved thermal-to-electrical efficiency.

The c-axis thermal conductivity, thermopower, and electrical resistivity for the Stage-5 K-GIC are given in Figures 6, 7, and 8, respectively. Each figure has three regions, namely - (a) experimental data - solid line, temperature range from 2-300 K, (b) temperature extrapolated region - dashed line, temperature range from 300 - 2000 K, and (c) combined stage and temperature extrapolated region - dotted line, temperature range from 300 - 2000 K. These three regions will be discussed individually.

Experimental Data Region

It is evident from the experimental data that intercalation makes a pronounced reduction in c-axis thermal conductivity (see Figure 6). From Figure 7, it is evident that the c-axis thermopower increases linearly with temperature. The c-axis electrical resistivity of potassium intercalated graphite drops sharply with temperature as expected (see Figure 8).

Experimental Extrapolation Region

The temperature region of prime interest for energy conversion lies between 300 K and 1500 K. The individual thermoelectric parameters are extrapolated as shown in the dashed lines in Figures 6, 7, and 8. In each case, an attempt was made to extrapolate straight lines along a path consistent with the low temperature data.

Actually, these temperature extrapolations are based on somewhat more information than is evident from the figures. For example, the slope of the thermal conductivity extrapolation in Figure 6 is consistent with that of pyrolytic graphite at the higher temperatures. In the thermopower extrapolation, the linear relationship with temperature is in agreement with an analytical model developed by Huffman as well as the form of the equation that Sugihara (Ref. 9) has derived for the thermopower in GICs. Sugihara has stated that thermopower should stay linear with temperature to 2000 K.

Stage Extrapolation

Clearly, an important factor that can limit TTC output in a Stage-5-K-GIC is that many of the pristine carbon layers are parasitic to the energy conversion mechanisms. This statement can be appreciated more readily by referring to Figure 9 which divides the TTC unit cell length, into two parts - the sandwich section and the bulk section. The sandwich section consists of the intercalant layer and the two boundary carbon layers. This is the active energy conversion region. The bulk section consists of all carbon layers that are not immediately adjacent to the intercalant layer. This is the parasitic energy conversion region where temperature drops contribute little to the output emf and the bulk resistance consumes power.

Thermal Conductivity and Thermopower Stage Extrapolation

To obtain a physical feel, assume a TTC element with a length, l_E, of 0.5 cm for a Stage-5 K-GIC. Further, assume a hot junction temperature, T_H, of 1500 K and a cold junction temperature, T_C, of 500 K. Thus the number of TTC unit cells, N, is given by

$$N = l_E/I_c$$
$$= (0.5\ \text{cm})(10^8\ \text{A/cm})/(18.79\ \text{A})$$
$$= 2.66 \times 10^6$$

Idealizing to a constant thermal conductivity, the temperature drop across an individual TTC unit cell, ΔT_u, is given by

$$\Delta T_U = (T_c - T_a)/N$$
$$= (1500\ \text{K} - 500\ \text{K})/2.66 \times 10^6\ \text{cells}$$
$$= 3.76 \times 10^{-4}\ \text{K/cell}$$

The heat fluxes through the sandwich and bulk sections of the TTC unit cell are identical. From Figure 9 we can write

$$q/A = (T_a - T_c)/[d_s/k_s + d_B/k_B]$$
$$= k_c\,(T_a - T_c)/(d_s + d_B) \qquad (2)$$

where T_a, T_c, d_s, and d_B are evident from Figure 9 and k_s and k_B are the thermal conductivities of the sandwich and bulk sections, respectively. The measured c-axis thermal conductivity is given by k_c. One can solve equation 2 to give

$$k_s = d_s/[(d_s + d_B)/k_c - d_B/k_B] \qquad (3)$$

For K-GICs, d_s and d_B are known as soon as the stage, n, is specified. If one makes the approximation that

$$k_B = k_{HOPG}$$
$$= 2 \times 10^{-2}\ \text{W/cm-K @ 1000 K}$$

then one may calculate k_s. Recall that for a Stage-5 K-GIC,

d_s = 5.35 A
d_B = 13.44 A
k_c = 0.0062 W/cm-K (Extrapolated value @ 1000 K)

Then, from equation 3

$$k_s = 5.35/[(5.35 + 13.44)/0.0062 - 13.44/0.022]$$
$$= 0.0022\ \text{W/cm-K}$$
$$k_s/k_B = 0.0022/0.022 = 0.1$$

so that the effective thermal conductivity across the sandwich layer is only one-tenth of the bulk layer. Since the heat flux through a TTC element of cross sectional area, A is identical through both sandwich and bulk regions of the unit cell, a temperature distribution across the TTC unit cell can be constructed as shown in Figure 10. These calculations indicate that about 80 percent of the temperature difference across the TTC unit cell occurs across the sandwich region. Therefore, decreasing the stage number can markedly decrease the element conductivity, k_c as shown in Figure 11.

A corresponding analysis by Huffman and another model by Sugihara indicate that thermopower for GICs is expected to be linear in temperature and a weak function of stage number (as shown in Figure 12).

Electrical Conductivity Stage Extrapolation

Fortunately, data exists for the stage dependence of electrical conductivity (Figure 13). Potassium intercalation of graphite has a remarkable effect on its electrical conductivity. The ratio of room temperature electrical conductivities is

$$\sigma_{c1}/\sigma_{HOPG} = 1940\ (\Omega\text{-cm})^{-1}/8.3\ (\Omega\text{-cm})^{-1} = 234$$

Additional insight may be obtained by applying the elementary model used in extrapolating the K-GIC thermopower and thermal conductivity as a function of stage. The results of the analysis is shown in Figure 13.

Combined Stage and Temperature Extrapolated Region

If the temperature extrapolated Stage-5 K-GIC thermoelectric property data are multiplied by the ratios of Stage-1 to Stage-5 values from the elementary model, one obtains the dotted curves in Figures 6, 7, and 8.

The combined stage and temperature extrapolated figure-of-merit, $Z\overline{c}1$, for the Stage-1 K-GIC can be calculated from the "dotted line" thermoelectric property data in Figures 6, 7, and 8. The result is shown in Figure 14.

This figure-of-merit of Stage-1 K-GIC is compared to those of conventional thermoelectric materials at 873 K in Figure 15. Clearly, the comparison is most favorable.

Since the extrapolations in both temperature and stage number required to obtain $Z\overline{c}1$ are extended and based on an elementary model, the quite favorable results given in Figures 14 and 15 must be taken with a proverbial "grain of salt." However, the consistent results from the theoretical calculations and the extrapolated measurements are intriguing enough to justify an experimental study of the TTC. Such an investigation is in progress.

REFERENCES

1. N. Bohm, Quantum Theory, Prentice Hall, Englewood Cliffs, NJ. 1951.

2. Powell and Crasemann, Quantum Mechanics, Addison-Wesley, Reading, MA., 1961.

3. E.L. Wolf, Principles of Electron Tunneling Spectroscopy, Oxford University Press, New York, 1985.

4. F.J. Blatt, I. Zabala-Martinez, J. Heremans, and J-P. Issi, M. Shayegan, M.S. Dresselhaus, Physical Review B, 27, 2535 (1983).

5. M.S. Dresselhaus, Physics Today, 60 (1984).

6. M.S. Dresselhaus, G. Dresselhaus, Advances in Physics, 30, 139 (1981).

7. M.S. Dresselhaus, G. Dresselhaus, J.E. Fischer, and M.J. Moran, Intercalated Graphite, Materials Research Society Symposia Proceedings, Vol. 20, North Holland, NY., 1983.

8. F.A. Levy, Intercalated Layered Materials, D. Reidel Pub. Co., Boston MA., 1979.

9. K. Sugihara, Physical Review B, 29, 5872 (1984).

10. F.L. Vogel, Molecular Metals, ed. W. E. Hatfield, Plenum, NY, 1979.

11. N. Wada, Physical Review B, 24, 1065 (1981).

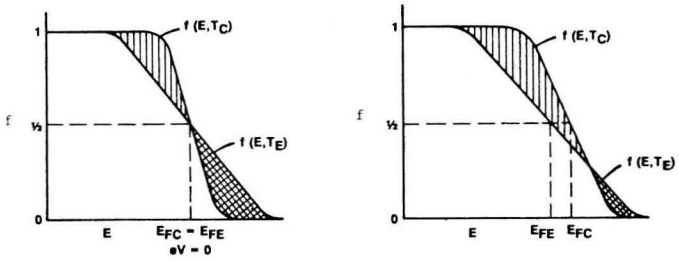

Fermi Function Versus E for eV = 0.

Fermi Function Vs. E for eV > 0.

Figure 1 Fermi Function Versus Electron Energy.

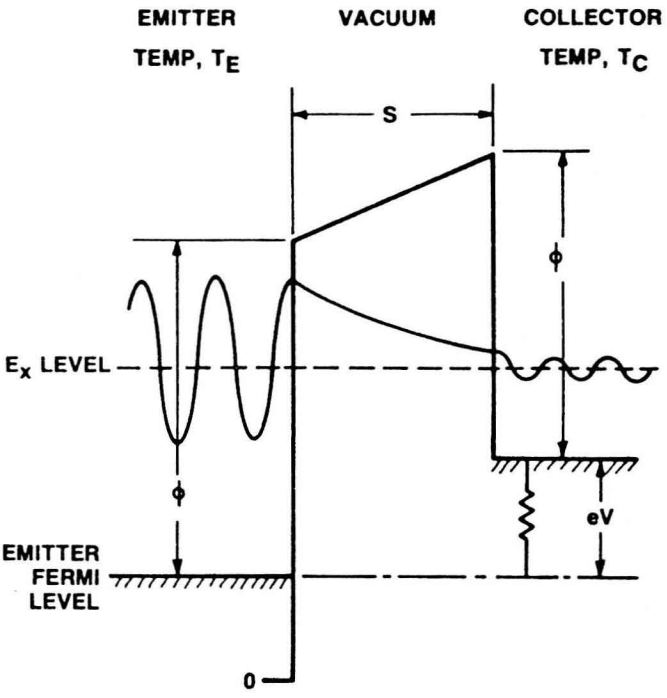

Figure 2 Potential Energy Diagram of Thermotunnel Converter.

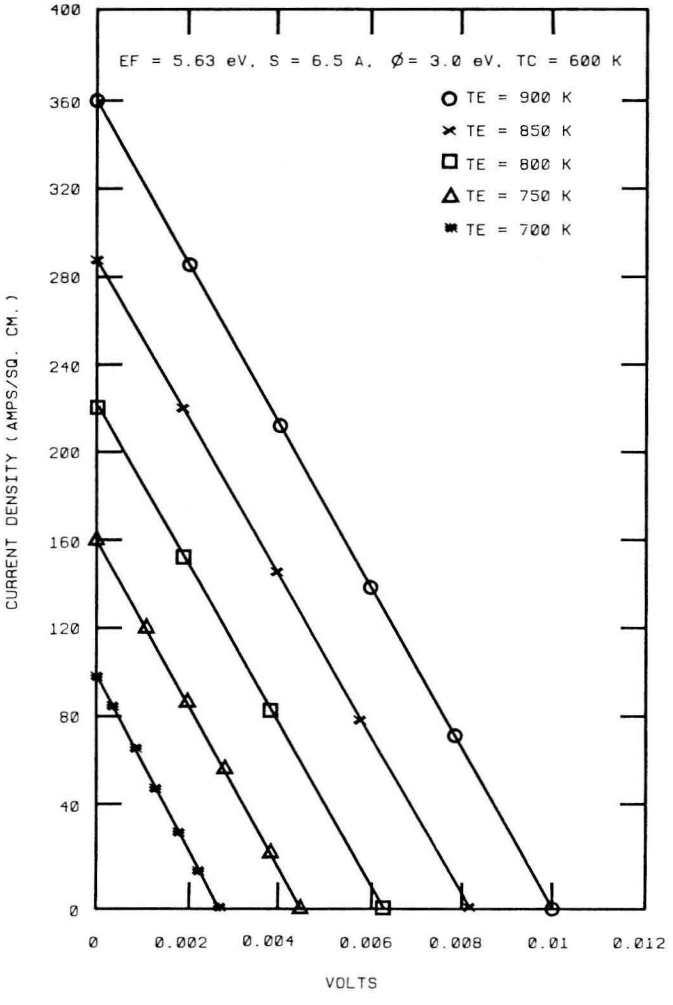

Figure 3 Current Density Versus Voltage, Parametric in Emitter Temperature.

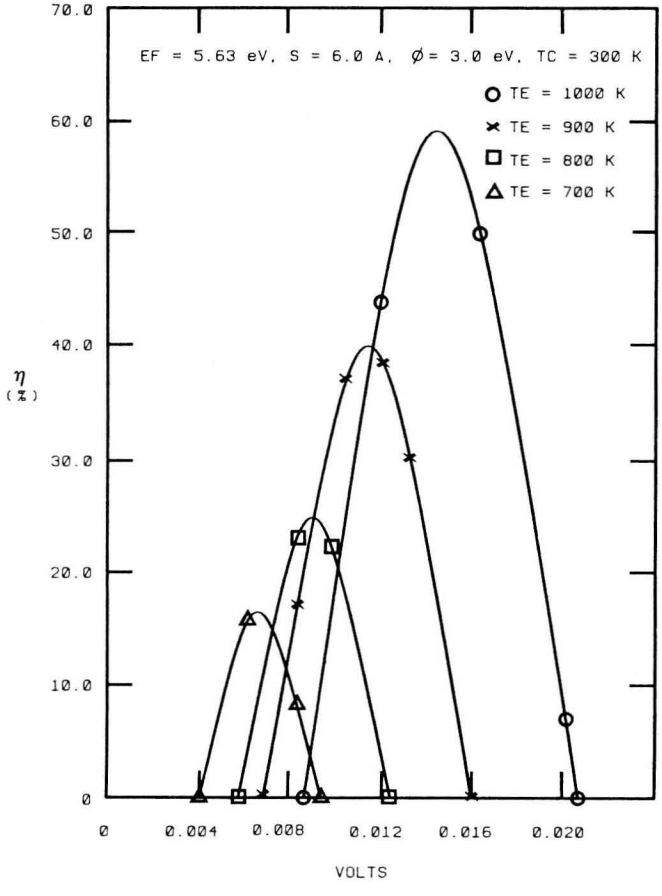

Figure 4 Efficiency Versus Voltage, Parametric in Emitter Temperature.

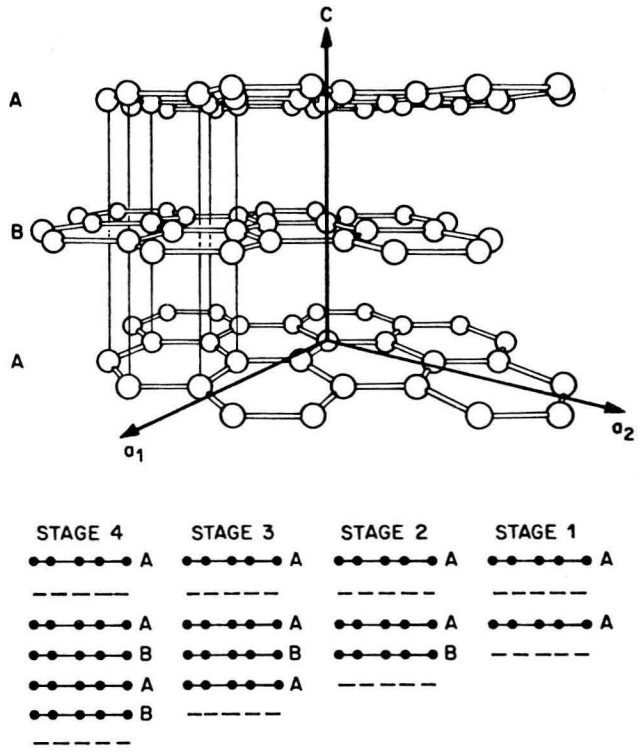

Figure 5 Crystal Structure of Pure and Intercalated Graphite.

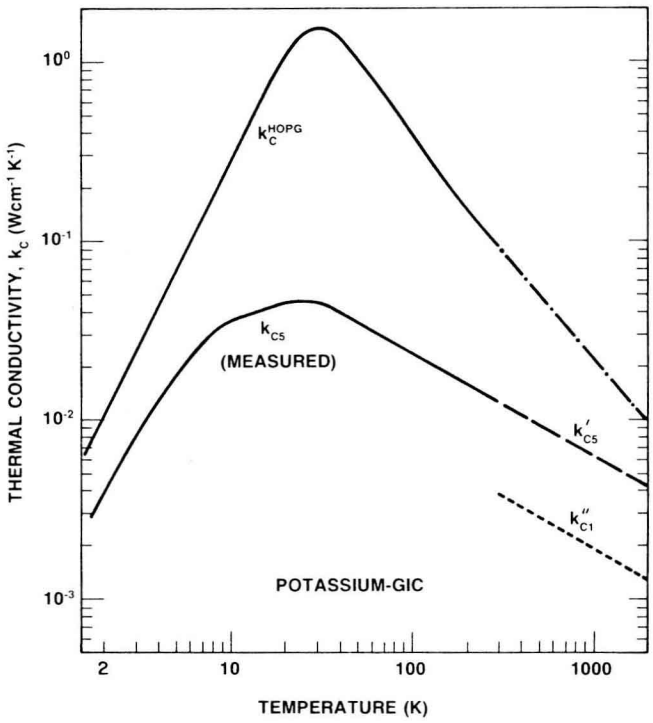

Figure 6 C-Axis Thermal Conductivity Versus Temperature.

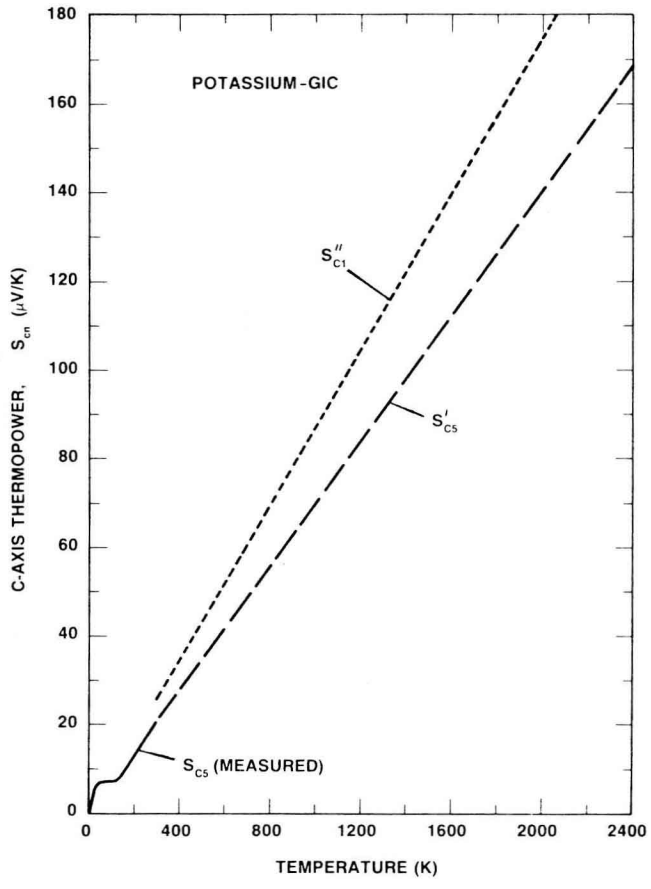

Figure 7 C-Axis Thermopower Versus Temperature. Solid Represents Experimental Data.

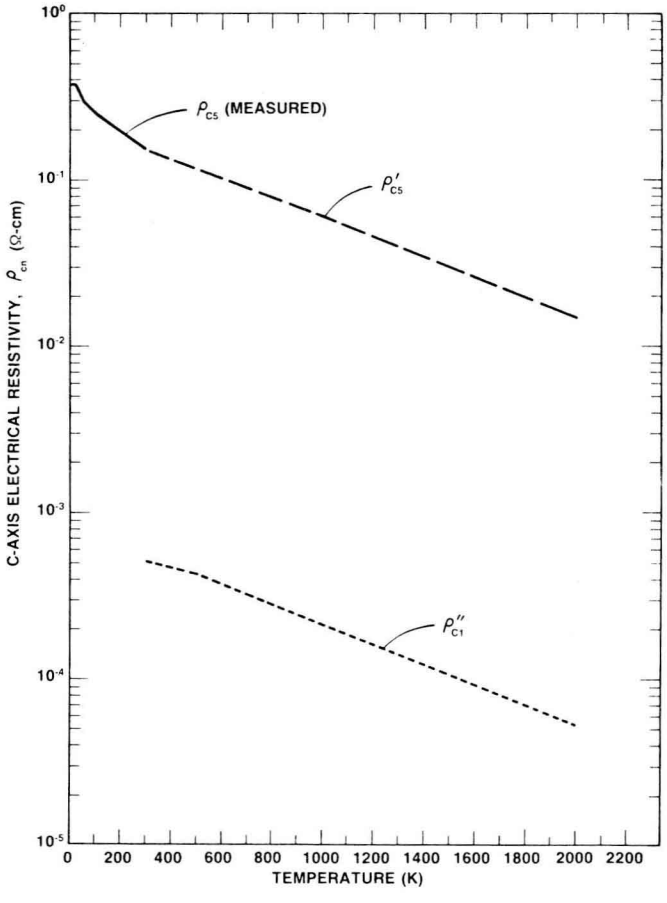

Figure 8 C-Axis Electrical Resistivity Versus Temperature.

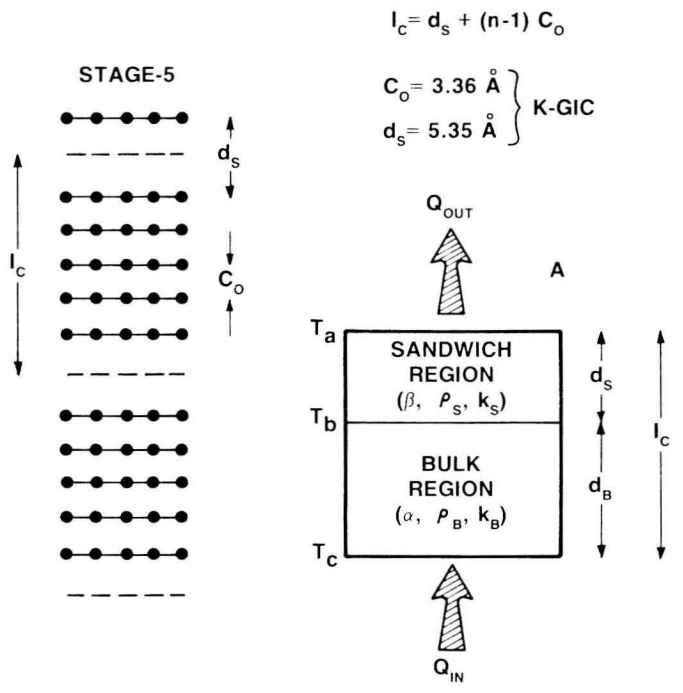

Figure 9 Thermotunnel Converter Unit Cell.

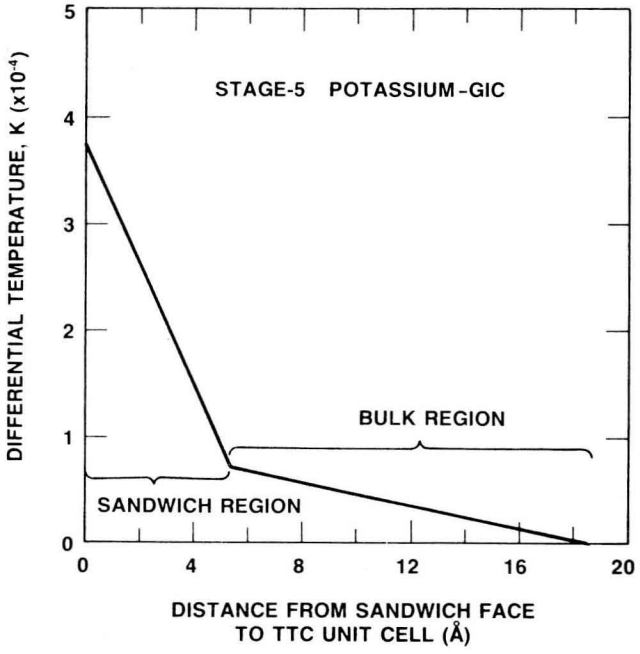

Figure 10 Temperature Difference Across Unit Cell.

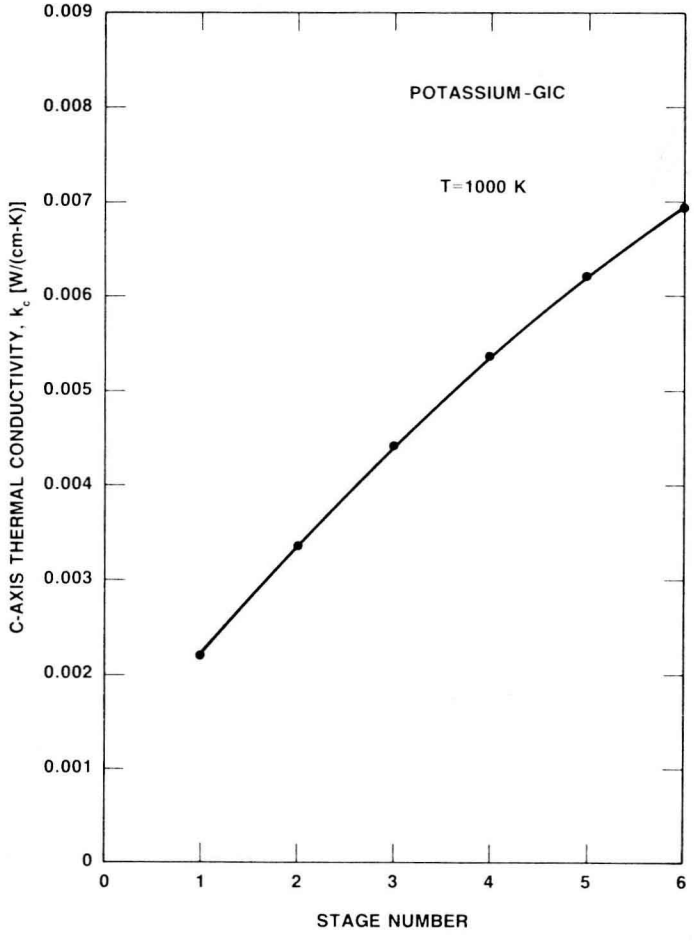

Figure 11 Extrapolated C-Axis Thermal Conductivity as a Function of Stage Number.

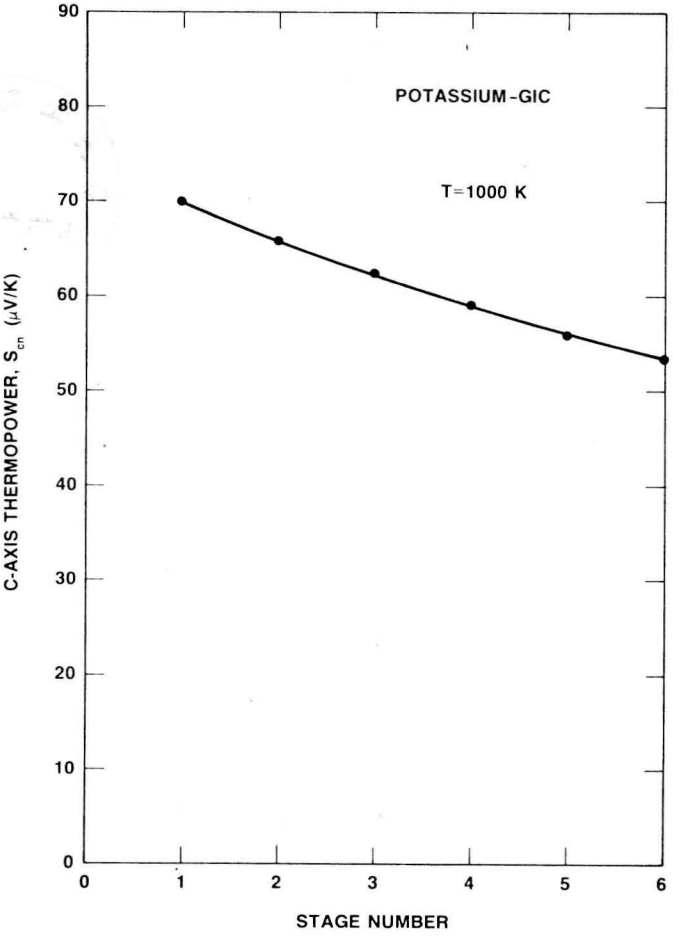

Figure 12 Extrapolated C-Axis Thermopower as a Function of Stage Number.

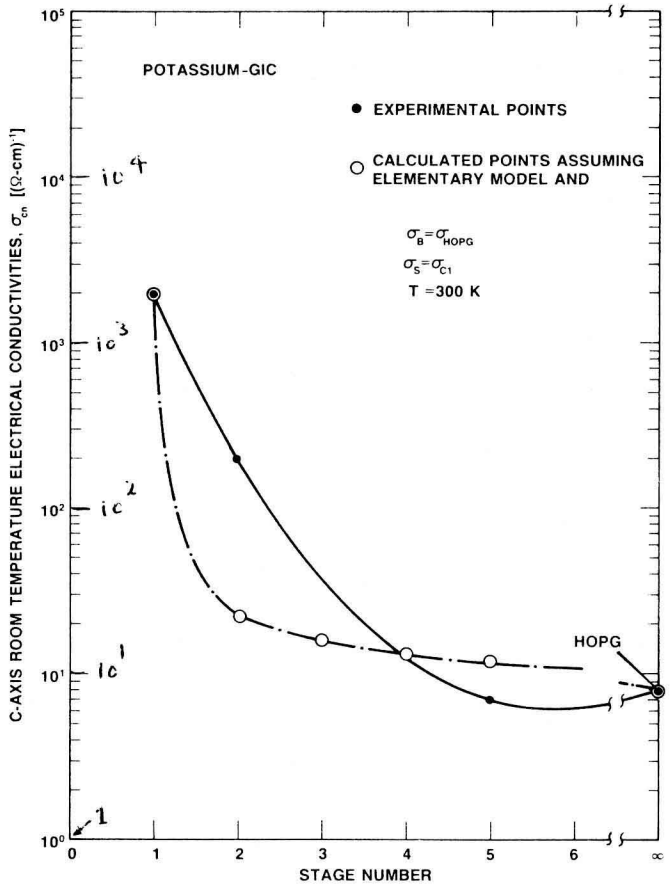

Figure 13 C-Axis Electrical Conductivity as a Function of Stage Number.

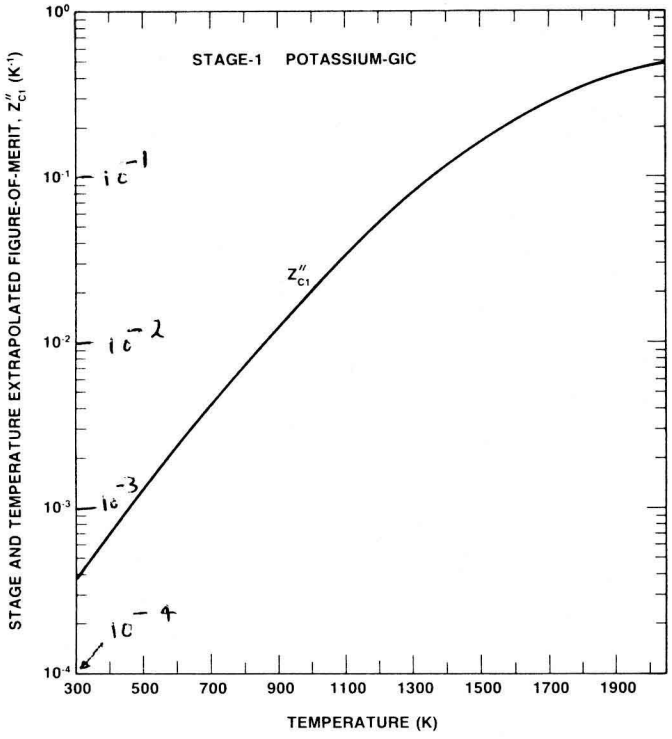

Figure 14 Stage and Temperature Extrapolated Figure-of-Merit for Stage-1 K-GIC.

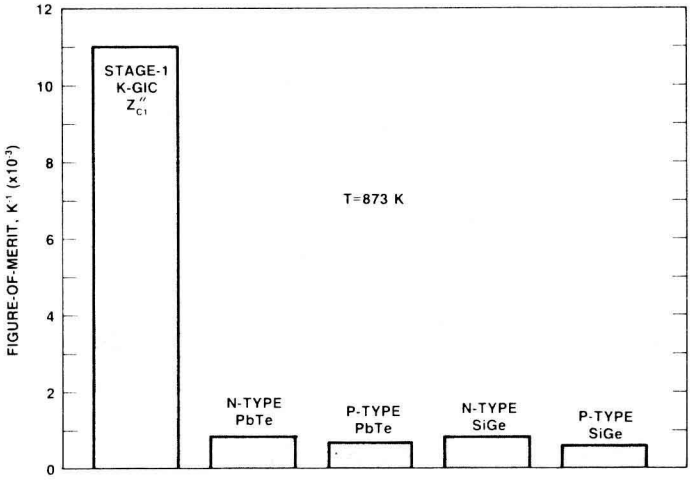

Figure 15 Figure-of-Merit of Stage-1 K-GIC Compared to Those of Conventional Thermoelectric Materials at 873 K.

ELECTRICAL AND THERMAL TRANSPORT IN LANTHANUM TELLURIDE

C. Vining*, C. Wood*, J. Parker*, A. Zoltan*, L. Danielson**, and M. Alexander**

*Jet Propulsion Laboratory, California Institute of Technology, Pasadena, CA 91109
**Thermo Electron Corporation, Waltham MA 02254

ABSTRACT

High temperature electrical and thermal transport properties are reported for Th_3P_4-type $LaTe_y$ with nominal composition between y=4/3 and y=3/2. Electrical resistivity, Seebeck coefficient, Hall coefficient, Hall mobility and thermal conductivity data are presented between 300 K and 1300 K. The figure of merit is found to increase with increasing temperature and exhibits a peak of about 1 x 10^{-3}/K at 1200 K as a function of composition for y=1.46. Simple parametric relations are presented which describe the Hall factor, electrical resistivity, Seebeck coefficient, and thermal conductivity over the entire temperature and composition range studied.

INTRODUCTION

Rare earth chalcogenides with the Th_3P_4 defect structure are promising n-type thermoelectric materials for high temperature electrical power generation. Values for the figure of merit ($Z=S^2/k\rho$) from 0.42x10^{-3} [1,2] to 1.0x10^{-3} at 1300 K have been reported [3] for the lanthanum telluride system. The high figure of merit values result in part from the relatively high effective mass and Hall mobility values and relatively low thermal conductivity values [1]. Previous studies, however, have not covered the entire single phase region with systematic results. In order to determine the composition which yields the optimum figure of merit, a systematic study of all of the high temperature transport properties has been undertaken covering the entire composition range. Each transport property has been found to vary in a systematic and physically reasonable way as a function of nominal composition.

EXPERIMENTAL DETAILS

Lanthanum telluride samples were prepared by reaction of stoichiometric mixtures of high purity lanthanum and tellurium in sealed quartz ampules, followed by melting in closed tungsten crucibles. The resulting slugs were ground and vacuum hot pressed. The electrical resistivity was determined from 300 K to 1300 K using a four probe dc technique simultaneously with a differential Seebeck coefficient technique, described elsewhere [4]. Further details on sample preparation, high temperature electrical resistivity and Seebeck coefficient results are described in an accompanying paper in these proceedings [5]. The thermal conductivity was calculated from thermal diffusivity and heat capacity data determined simultaneously using a flash technique between 600 K and 1300 K [6]. Electrical resistivity and Hall coefficient measurements were performed between 300 K and 1200 K using a switched dc van der Pauw's technique [7].

RESULTS

All of the transport properties of $LaTe_y$ are strong functions of the composition, y. An accurate measure of the composition is therefore essential to an understanding of the transport properties. In this study, the value of y refers to the nominal composition as determined by the ratio of tellurium to lanthanum employed in the preparation procedure. The nominal carrier concentration (n_y) is given by

$$n_y/n_o = (12/y - 8) \qquad (1),$$

where $n_o = 4.49 \times 10^{21}$ is the carrier concentration of the fully filled structure. Since the nominal composition is difficult to control, calculated n_y values may provide an inaccurate estimate of the actual carrier concentration, particularly for low carrier concentration samples with y near 1.5. Hall coefficient (R_H) measurements provide a direct estimate of the carrier concentration (n), if